

Fast Integrated Spectra Analyzer: A New Computational Tool for Age and Reddening Determination of Small Angular Diameter Open Clusters

ALEJANDRO BENÍTEZ-LLAMBAY

Instituto de Astronomía Teórica y Experimental, Observatorio Astronómico de Córdoba, Universidad Nacional de Córdoba,
Laprida 854, 5000, Córdoba, Argentina; alejandrobl@oac.uncor.edu

JUAN J. CLARIÁ

Observatorio Astronómico, Universidad Nacional de Córdoba, Laprida 854, 5000, Córdoba, Argentina;
claria@oac.uncor.edu

AND

ANDRÉS E. PIATTI

Instituto de Astronomía y Física del Espacio, CC 67, Suc. 28, 1428, Ciudad de Buenos Aires, Argentina; andres@iafe.uba.ar

Received 2011 September 11; accepted 2011 December 20; published 2012 February 9

ABSTRACT. We present a new algorithm called “Fast Integrated Spectra Analyzer” (FISA) that permits fast and reasonably accurate age and reddening determinations for small angular diameter open clusters by using their integrated spectra in the (3600–7400) Å range and currently available template spectrum libraries. This algorithm and its implementation help to achieve astrophysical results in shorter times than from other methods. A brief review is given of the integrated spectroscopic technique applied to the study of open clusters, as well as the basic assumptions that justify its use. We describe the numerical algorithm employed in detail, show examples of its application, and provide a link to the code. Our method has successfully been applied to integrated spectroscopy of open clusters, both in the Galaxy and in the Magellanic Clouds, to determine ages and reddenings.

1. INTRODUCTION

One of the main questions posed by stellar astrophysics has been, and continues to be, the formation and evolution of the Milky Way Galaxy. Thanks mainly to many determinations of chemical abundances, both for individual stars and for stellar systems in the Galaxy, remarkable advances in the understanding of these processes have taken place during the last four decades. However, in spite of these advances, a variety of issues related to Galactic evolution are not yet fully understood. These include such topics as the history of stellar formation, the initial mass function, and the processes of chemical enrichment. Any way to increase our knowledge of these subjects through observations of astronomical objects is obviously justified.

Observations of star clusters can be particularly useful. First, it is common knowledge that the Galactic open and globular clusters cover most of the age and chemical abundance ranges known in the universe, and one can therefore consider the Galactic cluster system as representative of the general stellar population in terms of age and metallicity. Second, the determinations of the fundamental parameters of open clusters (OCs) has undeniable importance in better understanding the structure and chemical evolution of the Galactic disk.

In general, such parameters as interstellar reddening, distance, age, and even metallicity may be determined more easily and more accurately for star clusters than for isolated stars. The

determination of such parameters in OCs has usually been based on color-magnitude diagrams (e.g., Lyngå 1987; Hasegawa et al. 2008) and/or on photometric and spectroscopic studies of individual stars (e.g., Clariá et al. 2006; Mermilliod et al. 2001). However, for small angular diameter OCs, the integrated spectra can be used to infer those properties (e.g., Santos & Bica 1993). Observations of cluster integrated spectra have been carried out at the Observatorio Astronómico de Córdoba (Argentina) over the past decade. Analysis of some of these data has demonstrated that this is a good way to determine cluster parameters with comparatively short observing times (see, e.g., Ahumada et al. 2000, 2001, 2002, 2007; Piatti et al. 2005; Palma et al. 2008a, 2008b; Talavera et al. 2010).

Given that the integrated spectra technique represents an efficient way to increase the amount of observational data for OCs, we want to have a method that systematically and automatically analyzes such data and yields astrophysical results. This article describes the development of the algorithm used to develop our computational tools to analyze the sample of previously unstudied small angular diameter Galactic OCs, which have been observed at the Complejo Astronómico El Leoncito (CASLEO, Argentina) to determine ages and reddenings.

This article is organized as follows: Section 2 discusses the main ideas that justify the use of integrated spectroscopy to estimate ages and reddenings of small angular diameter OCs.

Section 3 first describes two different methods of determining the $E(B - V)$ color excess that affects a star cluster's integrated emitted flux. We next show how these two methods can be combined in order to simultaneously determine the age and reddening of an OC. Finally, we present in this section a new algorithm, "Fast Integrated Spectra Analyzer" (FISA), that is suitable for a fast determination of the two mentioned OC parameters. Section 4 gives two examples of how FISA works in different cases. Section 5 summarizes our main conclusions.

2. STELLAR POPULATION AGES

It is currently possible to compute the spectral energy distribution of a star from the theory of stellar atmospheres in detail. If we consider a certain number of stars in a given area of space and we know the mass, the chemical composition, and the evolutionary stage of each star, it is possible to determine the spectrum of the light emitted by each star and, therefore, what the integrated spectrum of all the stars will be. This approach to determining the energy output for astronomical sources in which it is impossible to resolve their individual components is called stellar population synthesis theory (see, e.g., Cid Fernandes et al. 2005 and references therein). Typically, this theory is used in interpreting the spectra of galaxies whose stars are not resolved.

For a stellar cluster one must take into account that the distribution of stellar energies changes through time. The more massive stars leave the main sequence before less massive ones and, in the course of time, this causes a decrease in the number of blue stars in the cluster relative to the red ones. Thus, the integrated spectral energy distribution of a cluster constitutes a parameter that changes over time, gradually becoming redder, and it seems reasonable that this parameter can be an indicator of cluster age.

One can hypothesize that at any point in its history a cluster is characterized solely by its integrated light. This leads to the idea of building a library of integrated spectra templates for star clusters in different evolutionary stages that can be used for interpreting observations. There are two ways of doing so. The first consists of building the templates synthetically based on the stellar evolution theory (e.g., Bessell et al. 1998; Kurucz 1992). The second way consists of observing a large number of OCs whose ages were determined by direct methods (e.g., using color-magnitude diagrams) and, from these, developing the library of template spectra (e.g., Santos et al. 1995; Piatti et al. 2002; Ahumada et al. 2007).

2.1. Stellar Population Synthesis

The physical properties of a star at any given stage in its life can be described by an appropriate stellar model that can be computed if the star's initial mass and metallicity are known. As we can only measure the radiative fields coming from the stars, luminosity and effective temperature seem to be the most

appropriate theoretical properties on which to focus. A star's evolution is represented by an evolutionary track in the L versus T_e diagram. These two parameters are related to absolute magnitude and color, respectively, and therefore evolutionary tracks provide the basis for understanding the observed Hertzsprung-Russell (HR) diagrams.

There are many computational codes available in the astronomical literature for computing stellar models and stellar evolution under different assumptions and deriving evolutionary tracks of stars in the L versus T_e diagram. The tracks are often combined to obtain isochrones that represent the locus in the diagram for a group of stars that formed together. Examples can be seen in Lejeune & Schaerer (2001) and Girardi et al. (2002).

According to stellar population synthesis theory, the energy distribution of an unresolved star cluster will be the sum of the individual contributions of each star. There are essentially two different approaches to determining a cluster's age by using integrated spectroscopy. One is to compare the integrated radiation with the predictions of stellar evolution theory. These so-called evolutionary population synthesis methods aim to reproduce the observed spectrum by combining information for the entire stellar system using libraries of evolutionary tracks and stellar spectra with prescriptions for the initial mass function (IMF), star formation rate, and chemical histories. The main advantage of this approach is the possibility of progressing through a large group of parameters to generate synthetic spectra for all the required conditions. In practice, very sophisticated stellar atmospheres codes are used (e.g., Bessell et al. 1998; Kurucz 1992). Once a synthetic spectrum library is available, the integrated spectrum of a studied cluster can be fit by making a linear combination of the library's synthetic spectra.

The second approach is to apply empirical population synthesis methods. These aim at reproducing the observations by means of linear combinations of observed spectra of individual stars, of individual clusters, etc. Three different empirical methods have been used to try to characterize cluster age by using integrated spectroscopy:

1. The first method consists of obtaining spectra of nearby stars with known bolometric magnitudes M_b , effective temperatures T_e , and metallicities Z . Once these spectra are available, the particular spectrum of a star having other M_b , T_e , and Z values can be determined by means of a simple interpolation. Spectral libraries suitable for this can be seen in, for example, Gunn & Stryker (1983), Scalo (1998), and Le Borgne et al. (2003). This technique can also be used to characterize a stellar population—using linear combinations of the interpolated spectra—and it has been used to determine age and metallicity of OCs (e.g., Dias et al. 2010). The method is somewhat limited, however, because good-quality spectra with well-determined parameters are available only for stars in the solar neighborhood, which constitute a very limited stellar sample.

2. The second empirical method for characterizing a cluster age by using integrated spectroscopy was explored by Bica & Alloin (1986). They found that the equivalent widths of the Balmer lines in a cluster integrated spectrum are related to its age. They showed, however, that in most cases there is not a unique relationship between these two parameters. For this reason, this equivalent width method is not reliable to fully characterize a cluster age. Nevertheless, this method is of interest, because equivalent width determinations are practically reddening independent, which permits a cluster age to be estimated without knowing the reddening.

3. The third approach consists of spectroscopically observing OCs to obtain a library of template spectra from clusters of known ages. Because a cluster's integrated energy distribution is determined by its evolutionary stage, the ages of clusters can be found by comparing the continuum shape and the strength of the various absorption lines in their integrated spectra with these features in the integrated spectra of OCs of known ages. It was this third approach that inspired Santos & Bica (1993) to start building a library of template spectra suitable for characterizing the evolutionary stages of Galactic and extragalactic clusters. It should be noted that, assuming the Galactic IMF is universal, it is not necessary to make any assumption about its form, because the IMF is essentially built into the template spectra.

Based on stellar population synthesis theory and on the arguments previously stated, we may conclude that there must be spectral properties inherent to different stellar populations. These properties are usually called "integrated spectral properties," since they reflect the properties inherent to a given population group as a whole.

During the last 10 years, many studies have been published that present results from using the preceding third method to investigate a good number of Galactic OCs (Ahumada et al. 2000, 2001, 2007; Palma et al. 2008a) and Magellanic Cloud star clusters (Ahumada et al. 2002; Piatti et al. 2005; Santos et al. 2006; Clariá et al. 2007; Palma et al. 2008b; Talavera et al. 2010).

In the present article, the aforementioned third method for determining cluster ages will be adopted to derive cluster ages.

2.2. Library of Template Spectra

Our approach to estimating ages of OCs from their integrated spectra is largely based on the third empirical method described in § 2.1. We therefore present the basis on which we develop our method of age determination using template spectrum libraries of OCs.

Star cluster integrated spectra represent a very important link between the study of stellar populations of galaxies and individual stars. Seen in this way, observations of the integrated radiation of unresolved stellar sources have an undeniable significance. In addition, the determination of reddenings, ages, and even metallicity of clusters can be performed more easily and more accurately than for individual stars.

Piatti et al. (2002) constructed a library of OC integrated spectra representing stellar populations of different ages. The method they used consisted of combining reddening-corrected spectra of clusters of practically the same age τ , i.e., those within a small interval of age $\Delta\tau$. The individual spectra were averaged, weighting them according to the square of their signal-to-noise ratios (S/N), to produce a single template spectrum having a good S/N. When each template was built, it was ensured that the continuum distribution and the spectral absorption features of the cluster spectra used to create such a template were very similar. In this way, a set of template spectra characterized by their different ages $\tau \pm \Delta\tau$ was obtained.

The result of Piatti et al. (2002) was 20 solar-metallicity template spectra in a wide age range, from those associated with gas emission until ages as old as a few billion years, generated from 47 integrated spectra of Galactic OCs observed mostly at CASLEO (Argentina). All the templates cover the same spectral range between 3600 Å and 7400 Å. Two new solar-metallicity templates corresponding to age groups of 4–5 Myr and 30 Myr were later created by Ahumada et al. (2007), while the templates for 20 Myr and for 3.5 Gyr were redefined using only spectra of high S/N, improving their quality. With these additions and improvements one now has available 22 high-S/N templates representing cluster evolutionary stages of 2–4, 4–5, 5–10, 20, 30, 40, 45–75, 100–150, 200–350, 500, 1×10^3 , and $3–4 \times 10^3$ Myr. Table 1 lists the notation for the available template spectra, along with the number of members associated with it. The first letter of the template indicates whether it corresponds to a young-age group (Y) or to an intermediate-age group (I). Within both the young- and intermediate-age groups, Piatti et al. (2002) used a second alphabetic character to identify different spectra and also included a third numeric character in the 2–4 and 5–10 Myr templates to differentiate cluster spectra corrected by different reddening values.

Following the procedure described by Clariá (2008), reddenings and ages of more than 50 small angular diameter Galactic OCs have been estimated (Ahumada et al. 2000, 2001, 2007; Palma et al. 2008a). Although metallicity has an impact on the spectra of OCs older than ~ 0.5 Gyr, the metallicity features in the spectra of these clusters in the $3600 \text{ \AA} < \lambda < 7400 \text{ \AA}$ spectral range are relatively weak (see, e.g., Bica & Alloin 1986), so they do not significantly affect the determination of the two derived parameters. The results are mainly based on comparison of the observed spectra with template spectra, but there was still some use of the relation between equivalent width and age found by Bica & Alloin (1986). This was because the task of comparing an integrated spectrum with each of the templates in a library often turned out to be very time-consuming and difficult when there was no previous hint on the cluster's age. As will be seen in § 3, the method of Clariá (2008) is based on the minimization of a certain function. Measurement of the equivalent widths containing the Balmer spectral features suggested where to start looking for this minimum, thus constraining the

TABLE 1
LIBRARY OF TEMPLATE SPECTRA TAKEN FROM PIAITI ET AL.
(2002) AND AHUMADA ET AL. (2007)

Name	Age range (Myr)	Members
Ya1	2–4	3
Ya2
Ya3
Yab	4–5	2
Ya1_WR	5
Ya2_WR
Ya3_WR
Yb1	5–10	3
Yb2
Yb3
Yb1_WR	6
Yb2_WR	6
Yb3_WR	6
Yc ^{1a}	20	2
Ycd	30	3
Yd	40	3
Ye	45–75	5
Yf	100–150	6
Yg	200–350	7
Yh	500	2
Ia	1000	4
Ib ^a	3000–4000	3

NOTE.—These templates are loaded in FISA. All template spectra have solar metallicity.

^aYc and Ib templates were redefined in Ahumada et al. (2007).

search. The age finally adopted for a studied cluster was, however, only the result from the template match method. In the procedure described in this article, we managed to avoid this step by automating the search for the template that best matches the reddening-corrected observed spectrum.

To summarize, in this section we have tried to demonstrate why it is reasonable that the spectrum radiation distribution of a particular stellar population can reflect its evolutionary stage. OCs may be considered pure stellar populations in the sense that all their stars were formed at the same time and have just about the same metallicity. Thus, it seems reasonable to suppose that their integrated spectra may provide information about their ages. In fact, when one deals with unresolved sources, it is only through their integrated spectra that one can investigate the astrophysical nature of the objects. Several examples of astrophysical applications of the integrated spectroscopic technique have been described by Clariá (2008). Thus far, we have described three different ways to determine the ages of stellar populations by using only their integrated light. We will now describe how to estimate both ages and reddenings for OCs from integrated spectroscopy.

3. AGE AND REDDENING DETERMINATION

It has been shown that it is possible to characterize the evolutionary stage of an OC from its integrated spectrum.

The spectrum, of course, may be affected by interstellar reddening, and we will now show that it is possible to derive OCs' reddenings using their integrated spectra. However, to determine both a cluster's age and its reddening through comparison with a template spectrum library implies finding a single fitting parameter, which we will call the “age-reddening” parameter. Physically, a cluster's age is independent of its reddening, but when a template spectrum library is used, one must find the most probable combination of both parameters (age and reddening). If the apparent interdependence between these two parameters is taken into account, one can establish a sound criterion for determining both age and reddening for OCs by using integrated spectroscopy.

3.1. Reddening Determination

In this section, we describe a way of determining the $E(B-V)$ color excess affecting the integrated emitted flux of a star cluster by a procedure we call the “average method.” This method allows us to automate age and reddening determinations for OCs.

3.1.1. The Average Method

The average method consists of being able to find a mean cluster reddening in the sense that will be explained later. This method demands fewer operations than other procedures and yields good results. The fundamental ideas are described next.

Let us consider a light source (star or star cluster) located somewhere in the Galaxy. The observed monochromatic flux at a given wavelength λ will be

$$F(\lambda) = F_0(\lambda)e^{-\gamma_\lambda E(B-V)}, \quad (1)$$

wherein $F_0(\lambda)$ is the object's original flux, $\gamma_\lambda = -0.4 \ln(10)\xi(\lambda)$, and $E(B-V)$ is the color excess. In this work $\xi(\lambda)$ is the Seaton (1979) interstellar extinction law.

For practical reasons, the flux is usually normalized by dividing it by the flux in a certain wavelength. Thus, the normalized equation renders

$$F'(\lambda) = F'_0(\lambda)e^{-\gamma'_\lambda E(B-V)}, \quad (2)$$

where it is now $F'(\lambda) = F(\lambda)/F(\lambda_0)$, $F'_0(\lambda) = F_0(\lambda)/F'_0(\lambda_0)$, and $\gamma'_\lambda = \gamma_\lambda - \gamma_{\lambda_0}$.

From the preceding equation, it can be noted that if the object's original flux is known, it is possible to find $E(B-V)$ and vice versa. Assuming we know $F'_0(\lambda)$, then

$$E(B-V) = -\frac{1}{\gamma'_\lambda} \ln G_\lambda, \quad (3)$$

wherein $G_\lambda = F'(\lambda)/F'_0(\lambda)$.

The left side of equation (3) can be taken to be a constant. The first factor on the right side certainly is not; consequently, the variations of G_λ and γ'_λ should be such that the $\ln G_\lambda$ to γ'_λ ratio is constant: i.e., equals $-E(B - V)$.

The noise in the flux measurements produced by photon counting affects the value of $E(B - V)$ determined in this way. It is therefore appropriate, from a physical point of view, to write equation (3) in the following way:

$$E(B - V)_i = -\frac{1}{\gamma'_{\lambda_i}} \ln G_{\lambda_i}. \quad (4)$$

This equation shows that a different $E(B - V)_i$ value corresponds to each λ_i . Moreover, as the difference between the reddening associated with various wavelengths are only the result of noise introduced during the measuring process, it is expected that such reddenings are random and there will be a predictable reddening distribution. We now establish what this distribution is like.

3.1.2. Color Excess Distribution

It is well known that, for each λ , the noise associated with the observed flux follows a Poisson distribution, since the flux measurement is made by counting photons. On the other hand, for very long integration times, the expected frequency of photon detection is very large. So the noise should resemble a normal distribution. Therefore, it is reasonable to accept that the observed flux belongs to a Gaussian distribution with a mean μ_λ and a standard deviation σ_λ . This information should be enough to fully characterize the color excess distribution. However, we will adopt a more intuitive way to derive it.

Assuming a theoretical reddened flux (without noise), the theoretical reddening from equation (3) must be

$$E(B - V)_0 = -\frac{1}{\gamma'_\lambda} \ln G_\lambda, \quad (5)$$

As mentioned, equation (5) is only true theoretically. However, if an actual G_λ determination has an associated uncertainty δG_λ , then equation (5) can be written as

$$E(B - V)_\lambda = -\frac{1}{\gamma'_\lambda} \ln [G_\lambda + \delta G_\lambda]. \quad (6)$$

Assuming the observations have a reasonably good S/N, we expect $\delta G_\lambda \sim 0$. It is then possible to express equation (6) to first order as

$$E(B - V)_\lambda = E(B - V)_0 - \frac{\delta G_\lambda}{G_\lambda} \frac{1}{\gamma'_\lambda}. \quad (7)$$

So, in this approach, the variations in measured $E(B - V)$ values come only from the measurement process and follow the adopted extinction curve.

In the visual spectral range, the γ_λ extinction curve is proportional to $1/\lambda$ so that the most probable reddening for each λ is

$$E(B - V)_\lambda = E(B - V)_0 - \frac{\delta G_\lambda}{G_\lambda} \frac{\lambda \lambda_0}{\alpha(\lambda_0 - \lambda)}, \quad (8)$$

where α is the proportionality constant whose value is $\sim 10^4 \text{ \AA mag}^{-1}$. Thus, we have shown that, for each wavelength, the $E(B - V)$ value we expect to measure rises in proportion to $(\delta G_\lambda \lambda_0)/(\alpha G_\lambda)$ and follows the $\lambda/(\lambda_0 - \lambda)$ curve.

A good way of applying this method is by defining a mean reddening $\langle E(B - V) \rangle$. This procedure is justified as follows. The mean reddening is defined as

$$\langle E(B - V) \rangle = \lim_{t \rightarrow \infty} \frac{1}{2t} \int_{-t}^t E(B - V)_\lambda d\lambda. \quad (9)$$

Although it might be expected that the $\delta G_\lambda/G_\lambda$ ratio slightly depends on the wavelength due to variations in instrumental sensitivity, to simplify the discussion we assume the ratio is independent of λ . It is then evident that, in the absence of systematic errors, δG_λ will cause the measured points to be above or below the $1/\gamma'_\lambda$ curve by chance. The associated $1/\gamma'_\lambda$ curve depends as much on the sign of δG_λ as on its absolute value. Owing to this fact, two consecutively measured points may be situated on fairly different curves if the sign of δG_λ changes. The consequence is that the measured points will populate a dense region in the $E(B - V)_\lambda$ versus λ diagram, corresponding to all possible curves proportional to $1/\gamma'_\lambda$, with their proportionality constants depending on the normalizing wavelength, on the α value, and on the $\delta G_\lambda/G_\lambda$ ratio. This is illustrated in Figure 1, where we compute $E(B - V)$ values using a spectrum that has been reddened and had noise added, as shown in Figure 2. It is clear that the measured points do populate the region of the allowed $1/\gamma'_\lambda$ curves. The average reddening over all points is 0.5, which agrees with the reddening that was applied to the original spectrum.

Since δG_λ is a random variable and the absolute value of $\delta G_\lambda/G_\lambda$ should suffer little change in a neighboring continuum, it is expected that the points measured on a determined curve proportional to $1/\gamma'_\lambda$ cancel with their opposite. In this way, they produce the net effect that the mean value of all points is $E(B - V)_0$. This occurs when we have the same number of points on both sides of the normalizing point. So, in absence of systematic errors, we expect that

$$\lim_{t \rightarrow \infty} \frac{1}{2t} \int_{-t}^t \frac{\delta G_\lambda}{G_\lambda} \frac{\lambda}{\lambda_0 - \lambda} d\lambda = 0. \quad (10)$$

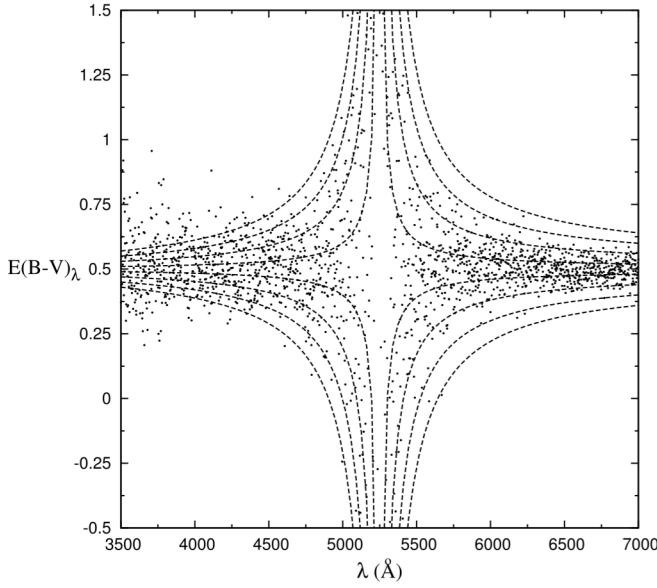


FIG. 1.—Derived $E(B - V)$ values (points) and four of the many possible theoretical distributions (dashed lines). The normalization wavelength is 5248 Å. The large scatter on the left is due to deviations from the standard $1/\lambda$ extinction curve.

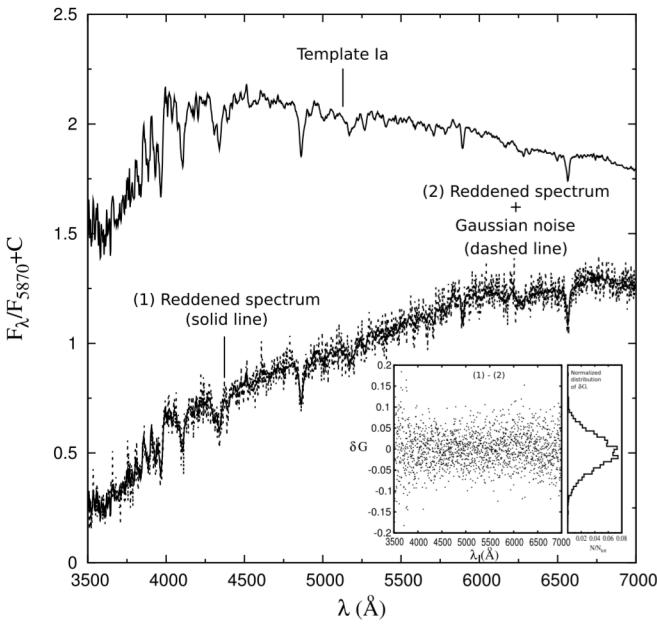


FIG. 2.—From top to bottom: The Ia template spectrum and the same spectrum now reddened by $E(B - V) = 0.5$ (solid line). Overlaid on the reddened spectrum is the spectrum that results from adding noise with a wavelength-independent standard deviation (dashed line). Also shown is the distribution of δG , defined as the difference between the fluxes of the reddened spectrum without noise and the one with noise added (small box).

In the case of a discrete distribution, the mean reddening is

$$\langle E(B - V) \rangle = \frac{1}{N} \sum_{i=1}^N E(B - V)_i, \quad (11)$$

where the subindex i indicates the measured reddening using the λ_i wavelength according to equation (4) and N is the number of analyzed spectral points.

The basic algorithm to determine reddening according to this method is the following:

1. Normalize both the original and the observed spectra at the mean value $\langle \lambda \rangle = (\lambda_{\max} - \lambda_{\min})/2$ to ensure that the number of points lying on both sides of the normalizing point are the same.
2. Compute the extinction curve $\gamma'_\lambda = \gamma_\lambda - \gamma_{\langle \lambda \rangle}$.
3. Determine the reddening for each λ according to equation (4).
4. Determine $\langle E(B - V) \rangle$ according to equation (11) and adopt the resulting value as the reddening affecting the spectrum.

In the next section, we describe another method to determine the reddening affecting an astronomical object. This one, together with the average method, will provide a powerful tool to simultaneously determine age and reddening of small angular diameter star clusters using integrated spectroscopy.

3.1.3. The χ^2 Method

Let us again consider equation (2), which relates the observed flux of an object with its reddening, its original flux, and the extinction law.

The original or intrinsic flux of the object is then

$$F'_0(\lambda) = F'(\lambda) e^{\gamma'_\lambda E(B - V)}. \quad (12)$$

Since the previous equation bears the same form as equation (2), it might be thought that to find $E(B - V)$, we can compute a sequence of fluxes whose terms result from the application of different reddenings to the observed flux. The basic idea consists of calculating as many cases as possible until one observed flux turns out to be equal to the object's original flux, assuming that the latter is known or given by a template spectrum. We can then construct the following sequence:

$$\begin{aligned} F'(\lambda) &= F'_0(\lambda) e^{-\gamma'_\lambda E(B - V)} \\ F'_1(\lambda) &= F'(\lambda) e^{-\gamma'_\lambda E(B - V)_1} \\ F'_2(\lambda) &= F'(\lambda) e^{-\gamma'_\lambda E(B - V)_2} \\ &\dots \\ F'_m(\lambda) &= F'(\lambda) e^{-\gamma'_\lambda E(B - V)_m}. \end{aligned} \quad (13)$$

If we find any $E(B - V)_j$ value for which we obtain $F'_j(\lambda) = F'_0(\lambda)$, we will have solved the problem of finding

the $E(B - V)$ color excess affecting the observed flux. Indeed, $E(B - V) = -E(B - V)_j$.

The most direct way to determine if $F_j(\lambda)$ is equal to the unreddened object original flux is to analyze the following normalized quadratic sum of the residuals:

$$\chi^2(E(B - V)_j) = \sum_{i=1}^N \frac{(F'_j(\lambda_i) - F'_0(\lambda_i))^2}{F'_0(\lambda_i)}. \quad (14)$$

Function χ^2 should have a minimum value within a closed reddening interval. We will not show here that this minimum is global and unique. Rather, we must somehow justify the $E(B - V)$ domain in which it should be sought. This will be explained later, when we give details about the method finally adopted for reddening determination. For now, the algorithm to find $E(B - V)$ following the χ^2 method is this:

1. Normalize both the observed and the original spectra in a given λ_0 .
2. Compute the extinction curve $\gamma'_\lambda = \gamma_\lambda - \gamma_{\lambda_0}$.
3. Build up the flux sequence equation (13) by dereddening the observed flux by different $E(B - V)_j$ values.
4. Compute the $\chi^2(E(B - V)_j)$ function.
5. Adopt the $-E(B - V)_j$ corresponding to the minimization of the $\chi^2(E(B - V)_j)$ function as the most probable reddening value.

3.2. Simultaneous Age and Reddening Determination

We have shown in previous sections how the reddening that affects an astronomical object can be determined using integrated spectroscopy. We assumed, however, that the object's original flux was already known. In this section, we will see that a reddening determination cannot be performed independently from the determination of the original flux. From a mathematical point of view, reddening depends on the original flux and vice versa, while from the physical point of view, there is no such degeneracy. A criterion must be established that allows an unambiguous determination of both the object's intrinsic flux and the $E(B - V)$ color excess affecting it.

When OCs are considered, as shown in § 2, the determination of the original flux can be carried out by using template spectra, which in turn leads to estimates of the cluster's age and reddening. But this is true only if the adopted extinction law is the correct one for the cluster's Galactic direction. We will next show how incorporating the average and χ^2 methods of reddening determination allows one to simultaneously determine the age and reddening of an OC.

3.2.1. Combining the Average and χ^2 Methods

If we believe that the observed flux of an object is related to an $E(B - V)$ that is well defined and unique for the object based on an erroneously selected k th template spectrum from

$$F'(\lambda) = F'_{0k}(\lambda)e^{-\gamma'_\lambda E(B-V)}, \quad (15)$$

then there will be a systematic error in the individual $E(B - V)_\lambda$ determinations. Indeed, in this case and in the absence of noise, equation (3) will not be valid, because a relation will not exist between G_λ and γ'_λ that permits $E(B - V)$ to be a constant. So, even if the noise in the observed flux is small, $E(B - V)_\lambda$ will not follow the distribution given by equation (8), because the large systematic component in G_λ will distort it. The distribution will become increasingly different from the one theoretically found as the difference between the k th template spectrum and the object's original flux increases. This behavior, illustrated in Figure 3, provides a way to ascertain if the adopted template spectrum is correct. If the observed reddening distribution can be matched by the one theoretically found, within certain limits, we may very well think that the adopted template is the right one. In case this is impossible to achieve, the template must be discarded and, consequently, the $E(B - V)$ value determined through the average method will not have any physical sense.

When the correct template spectrum is unknown, the χ^2 method demands finding the minimum value of the following function:

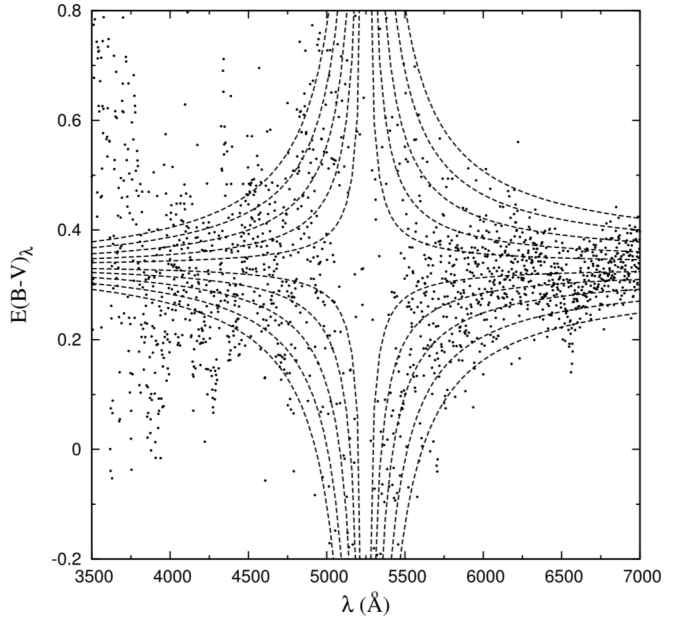


FIG. 3.—Distribution of computed $E(B - V)$ values (points) when a poorly matching template spectrum is used. The large and systematic deviations with respect to the theoretically expected curves (dashed lines) are mainly the result of the observed and template spectra having different spectral features. Thus, the differences between the observed and the template spectra are not being determined by the extinction.

$$\chi^2(E(B-V)_j; F'_{0k}) = \chi^2_{jk} = \sum_{i=1}^N \frac{(F'_j(\lambda_i) - F'_{0k}(\lambda_i))^2}{F'_{0k}(\lambda_i)}, \quad (16)$$

where F'_{0k} is the k th template spectrum.

The determination of the most probable template spectrum-reddening combination is performed considering two degrees of freedom: j and k . Given the nature of the problem, it is possible to fix k and vary j until $F'_j(\lambda) = F'_{0k}(\lambda)$. The combination of the most adequate j and k values can be found by minimizing χ^2_{jk} .

Following this procedure it is not difficult at all to minimize the χ^2_{jk} function by fixing k and varying j . We will have a minimum χ^2_{jk} value within the $E(B-V)_j$ domain searched for each k . The same procedure can be applied to all available k ; i.e., for all the existing template spectra, we will be able to characterize each k with a χ^2_{jk} value and finally choose the smallest of the χ^2_{jk} values among them. Although this method appears easy to apply, there remains the problem of selecting the initial value for each k from which we start the search for the χ^2_{jk} minimum. It is therefore possible to search the reddening interval from a very negative to a very positive value and to adopt the negative value that minimizes the function. However, we have to search with a fine enough screen to make sure that there is no other minimum in the interval. When a large sample of template spectra is handled, the described procedure may be rather slow.

A better approach is to use a combination of both the average and the χ^2 methods. Indeed, the average method involves the evaluation of at least one or two members of the sequence of equation (13) of the χ^2 method. Thus, an $E(B-V)$ value is quickly obtained, which serves as a starting point to look for the χ^2 minimum. It is only necessary to search for the minimum of the χ^2_{jk} function within a small interval ranging from $(\langle E(B-V) \rangle - \delta)$ to $(\langle E(B-V) \rangle + \delta)$ with a small δ value.

What will happen if one or more incorrect template spectra have been chosen? In this case, the reddenings resulting both from the average and the χ^2 methods will also be wrong, but this is not a problem because, even though those templates can be well characterized by a reddening value found by the average method, when the χ^2_{jk} minimum among all templates is found, the mistaken ones will be ignored. We should not expect that a template yielding mistaken results when the average method is used could be characterized by a χ^2 value lower than the template that would lead to right results. The only relevant templates are those for which the average method works correctly. It is precisely in these spectra in which the minimum χ^2_{jk} function will be found.

The method finally adopted in this work to determine reddening and age of small angular diameter OCs from their integrated spectra has the following steps:

1. Normalize the observed spectrum and that of the template at $\langle \lambda \rangle = (\lambda_{\max} - \lambda_{\min})/2$ so that the number of points on both sides of the normalizing point is the same.

2. Compute the extinction curve $\gamma'_\lambda = \gamma_\lambda - \gamma_{<\lambda>}.$
3. Determine $E(B-V)_i = -\ln(G_\lambda)/\gamma'_\lambda$ for each λ , where G_λ is the ratio between the normalized observed and template spectra.
4. Determine $\langle E(B-V) \rangle$ and adopt this value as the starting point for evaluating the function $\chi^2(E(B-V)_j).$
5. Adopt an interval between $\langle E(B-V) \rangle + \delta$ and $\langle E(B-V) \rangle - \delta$, wherein δ may be, for example, nearly equal to 1.
6. Adopt the $E(B-V)_j$ value that minimizes function χ^2_j as the cluster reddening.
7. Finally, follow steps 1 to 6 for each template spectrum and adopt, as the most probable cluster age and reddening, the j th reddening and the age of the k th template spectrum that globally minimize the χ^2_{jk} function.

This mixed procedure is much faster than simply applying the χ^2 method, since the search interval can be much smaller. It is also more reliable because we can make sure that the $E(B-V)$ that results from the search is quite close to the $E(B-V)$ expected from the average method. On the other hand, the mixed procedure is more reliable than just the average method, because the search for the minimum of the χ^2_{jk} function involves a global analysis of the spectrum, so localized effects do not have an influence on the final result. Such localized effects can be really troublesome when determining mean reddening. For these reasons, we believe that the mixed procedure should be the preferred method to use in characterizing a very large sample of template spectra and for determining ages and reddenings of small angular diameter OCs. The computational implementation of the method is relatively simple and allows one to fully systematize and automate age and reddening determination of small angular diameter OCs using the existing integrated spectrum template libraries.

3.3. Implementation of the Methods

The full implementation of the method described was done by developing the computational tool FISA.¹

Given an OC integrated spectrum covering the $3600 \text{ \AA} < \lambda < 7400 \text{ \AA}$ spectral range, FISA permits a fast and reasonably accurate determination of the cluster age and reddening by using the average and χ^2 methods. The Piatti et al. (2002) and Ahumada et al. (2007) spectral libraries are defined for this spectral domain, and these libraries are the ones used by FISA.

If the integrated spectrum in the optical range of an OC is available, FISA makes it relatively easy to quickly find the most probable age and reddening values. Basically, FISA works by either manually or automatically characterizing the observed spectrum with a reddening that minimizes the χ^2 function

¹ We release this application with its complete documentation at <http://sites.google.com/site/intspectroscopy>.

for each available template spectrum. FISA then selects, from among all the template spectra, the one that globally minimizes χ^2 . The results are the most probable values of reddening and age for the observed cluster.

Both the average and the χ^2 methods demand different operations between the observed spectrum and the selected template. These operations must be well defined for each wavelength. In general, the wavelength sampling of both spectra is not the same, so one must determine the template spectrum flux value in the observed spectrum wavelengths. This is done using cubic splines (e.g., Press et al. 2002), which permit the interpolation of the nominal flux value quite well. This procedure produces spectra that permit operations among them.

The template integrated spectra of Piatti et al. (2002) and Ahumada et al. (2007) have been reddening-corrected according to Seaton's (1979) law, so we use this same law in this work. Seaton's law includes only a few measured points in the visible region; hence, it is necessary to derive by interpolation a smooth extinction curve covering the region where the original spectrum was observed, which is also achieved using cubic splines.

4. PRACTICAL EXAMPLES

We now demonstrate the use of FISA through two practical examples. For the first we use observations of the OC ESO 502-SC19, which is located at a high Galactic latitude so that very small or nonexistent reddening is expected. For the second example, we use observations of the reddened OC Hogg 22 and then we apply FISA to see how well the reddening is recovered. This second example shows how FISA works for a reddened cluster.

4.1. ESO 502-SC19

ESO 502-SC19 has been studied by Bica et al. (2001) as one of a number of possibly dissolving OCs. They used the reddening maps published by Schlegel et al. (1998) to derive $E(B - V) = 0.05$ and, from measurements made on Digitized Sky Survey (DSS) images, determined such cluster parameters as Galactic coordinates and the apparent diameters of both the cluster's major and minor axes. Other than this work, ESO 502-SC19 has not been studied previously, either photometrically or spectroscopically.

The integrated spectrum of ESO 502-SC19 exhibits the features typical of an intermediate-age cluster. Using FISA, the best-matching template is Piatti et al. (2002) Ia, aged 1 Gyr. ESO 502-SC19 is found to be unaffected by reddening when the template-matching method is used, in good agreement with the small $E(B - V)$ value indicated by Schlegel et al.'s (1998) maps. The reddening distribution used to compute the mean reddening required by the average method and the expected theoretical curves are shown in Figure 4. The asymmetric systematic deviations at both sides of the normalizing point cause the derived mean reddening to deviate from the most probable redden-

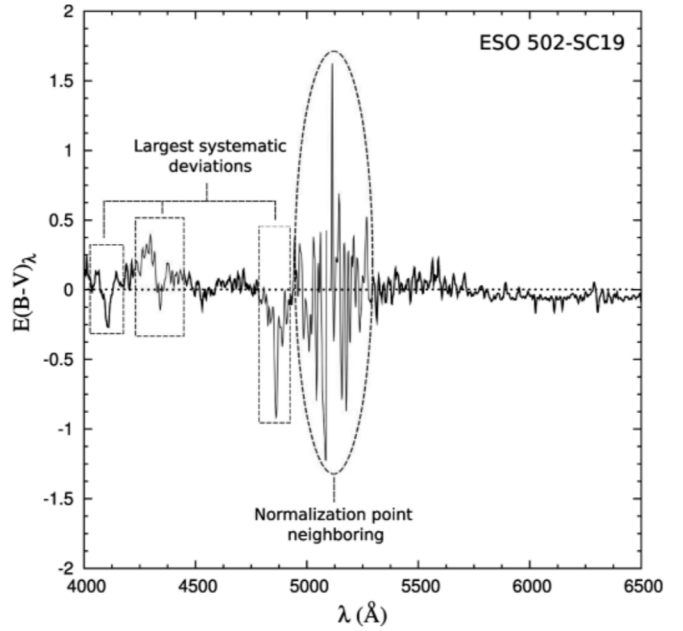


FIG. 4.—Distribution of $E(B - V)$ values from comparing the observed spectrum with the Ia template of Piatti et al. (2002). The systematic deviations at both sides of the normalizing point, due largely to spectral features that differ in the two spectra, cause the derived mean reddening to differ slightly from the most probable reddening value adopted for ESO 502-SC19.

ing for ESO 502-SC19. It is for this reason that, starting from the mean reddening, FISA computes the minimum value of the χ^2 function and thus finds the most probable $E(B - V)$ value. This procedure is performed for all available template spectra, choosing the one that globally minimizes the χ^2 function: namely, the Ia template with $E(B - V) = 0$. The observed spectrum, the adopted template, and the residual flux between both are shown in Figure 5.

4.2. Hogg 22

The sparse cluster Hogg 22 has been studied photometrically and spectroscopically. A compilation and discussion of these results can be seen in Ahumada et al. (2007). They showed that there is good agreement between the integrated spectrum of Hogg 22—neglecting the contribution of the bright star HD 150958 and applying a reddening of $E(B - V) = 0.55$ —and the template spectrum Yb1. Using FISA, one finds the integrated spectrum is again well fit with template Yb1 and with a similar reddening of $E(B - V) = 0.58$. The reddening results from the average method are shown in Figure 6. In spite of some systematic deviations, the mean reddening that resulted [$\langle E(B - V) \rangle \sim 0.52$] is very close to the value finally adopted. Figure 7 shows the template spectrum Yb1, the observed spectrum of Hogg 22, that spectrum corrected for the adopted reddening [$E(B - V) \sim 0.58$], and residuals in flux between the template and the corrected spectra.

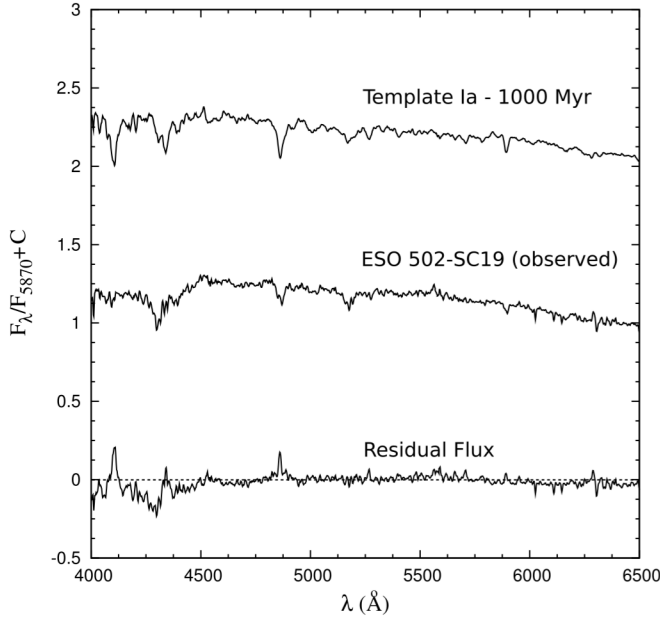


FIG. 5.—From top to bottom: The selected template spectrum, the spectrum of ESO 502-SC19, and the difference in flux difference between them computed through $(F_{\text{cluster}} - F_{\text{template}})/F_{\text{cluster}}$. Note the similarity between the larger values of flux differences and the anomalous $E(B-V)$ values in Fig. 4.

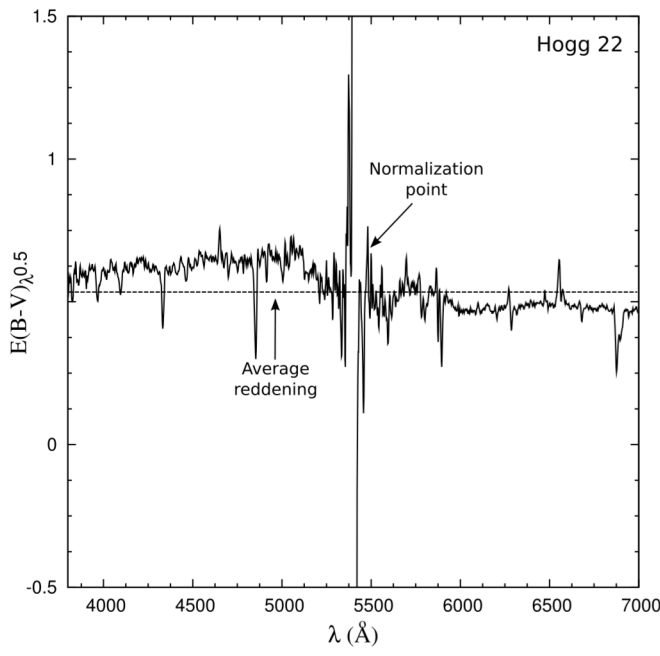


FIG. 6.—Distribution of the computed $E(B-V)$ values from comparing the observed spectrum of Hogg 22 with the Yb1 template spectrum of Piatti et al. (2002). As expected, there are large deviations near the normalization point. Despite this and the variations over the wavelength range, the reddening seems to be very well determined from the mean value produced by the average method.

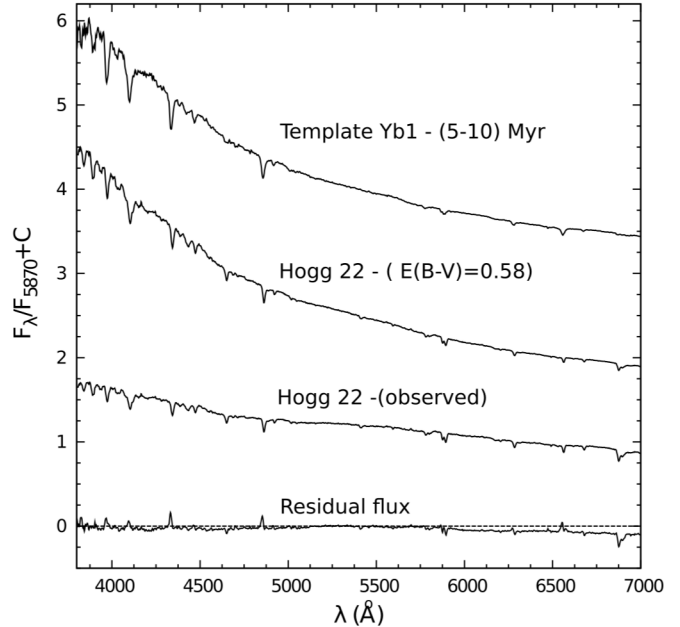


FIG. 7.—From top to bottom: The chosen template spectrum Yb1, the Hogg 22 spectrum dereddened by $E(B-V) = 0.58$, the original (observed) Hogg 22 spectrum and the flux difference between the dereddened spectrum and the template spectrum computed through $(F_{\text{cluster}} - F_{\text{template}})/F_{\text{cluster}}$.

5. CONCLUSIONS

Over more than a decade, the integrated spectroscopic technique has been developed and successfully applied at the Observatorio Astronómico of the Universidad Nacional de Córdoba (Argentina). Its application to different astronomical objects has led to interesting results in relation to OCs (e.g., Ahumada et al. 2001), globular clusters (e.g., Bica et al. 1998), planetary nebula (e.g., Bica et al. 1995), galaxies (e.g., Dutra et al. 2001), and even supernova remnants (e.g., Bica et al. 1995). However, during recent years, the technique has been mostly used to determine the fundamental properties of compact star clusters belonging both to our Galaxy (e.g., Ahumada et al. 2000) and to the Magellanic Clouds (e.g., Santos et al. 2006).

The main aim of this article was to describe a method in detail that not only allows us to systematize and automate the analysis of a large amount of integrated spectra, but also to obtain astrophysical results. We started by demonstrating in § 2 that the integrated radiation distribution of a stellar population is determined by its stage of evolution. Since OCs can be considered true stellar population units, because all their stars formed at the same time and they have about the same metallicity, their integrated spectra provide us with information about their ages. We then described three different approaches to the characterization of a cluster age from its integrated spectrum. We also presented some arguments validating the use of template spectrum libraries for interpreting an observed spectrum. As the existing dispersion in Galactic OC metallicities is small—especially

in young clusters—these stellar systems stand out as excellent candidates to be observed through integrated spectroscopy and to be analyzed using template spectra.

We presented in § 3 two different methods based on integrated spectroscopy to estimate age and reddening of small angular diameter OCs. The average method is quite useful as a starting point to estimate the reddening affecting a cluster. It was shown, however, that this method is not reliable by itself, since many systematic differences between the observed and the template spectra are to be expected when put into practice. We demonstrated that the errors introduced by these systematic effects can be removed by using the χ^2 method, which takes into account the overall spectrum shape so that variations over a small spectral range do not have a marked influence. We concluded that the safest option for estimating a cluster reddening from integrated spectra is to use a combination of both the average and χ^2 methods. The use of the average method permits a significant acceleration of the required calculations so that this approach is appropriate when dealing with a great number of clusters. Finally, we showed how this method can be practically implemented by deriving an extinction curve for the spectral range of the observed spectrum and interpolating the template spectrum data to obtain values at the measured points in the observed spectrum.

The theory developed in § 2, as well as the algorithms presented in § 3, allowed us to build a computational application that greatly facilitates the age and reddening determination from

integrated spectra of small angular diameter star clusters through the use of currently available integrated spectral libraries. We illustrated the use of this new tool, which we called “Fast Integrated Spectra Analyzer” (FISA), with two examples. We believe FISA represents a step forward in the formerly time-consuming task of analyzing integrated spectra. From now on, FISA will enable us to analyze large amounts of integrated spectroscopic data in relatively short times, thus simplifying the determination of age and reddening of small angular diameter OCs. In a forthcoming article, we will present the results obtained from integrated spectra obtained at CASLEO for about 50 OCs whose features are presently poorly known or practically unknown.

We thank the staff and personnel at CASLEO for hospitality and assistance during the observations. We would like to thank the anonymous referee for his or her helpful comments and suggestions that contributed to the improvement of the article. We also are indebted to W. Osborn, Yerkes Observatory, for carefully reading this manuscript and making some suggestions. The authors acknowledge use of the CCD and data acquisition system supported under NSF grant AST-90-15827 to R. M. Rich. We gratefully acknowledge financial support from the Argentinian institutions CONICET (Consejo Nacional de Investigaciones Científicas y Técnicas), FONCyT (Fondo para la Investigación Científica y Tecnológica), and SECyT (Universidad Nacional de Córdoba).

REFERENCES

- Ahumada, A. V., Clariá, J. J., & Bica, E. 2007, *A&A*, 437, 444
 Ahumada, A. V., Clariá, J. J., Bica, E., & Dutra, C. M. 2002, *A&A*, 393, 855
 Ahumada, A. V., Clariá, J. J., Bica, E., Dutra, C. M., & Torres, M. C. 2001, *A&A*, 377, 845
 Ahumada, A. V., Clariá, J. J., Bica, E., & Piatti, A. E. 2000, *A&A*, 341, 79
 Bessell, M. S., Castelli, F., & Plez, B. 1998, *A&A*, 333, 231
 Bica, E., & Alloin, D. 1986, *A&A*, 162, 21
 Bica, E., Clariá, J. J., Bonatto, C., Piatti, A. E., Ortolani, S., & Barbuy, B. 1995, *A&A*, 303, 747
 Bica, E., Geisler, D., Dottori, H., Piatti, A. E., Clariá, J. J., Jr., & Santos, J. F. C. 1998, *AJ*, 116, 723
 Bica, E., Santiago, B. X., Dutra, C. M., Dottori, H., & de Oliveira, M. R. 2001, *A&A*, 366, 827
 Cid Fernandes, R., Mateus, A., Jr., Sodré, L., Stasinska, G., & Gomes, J. M. 2005, *MNRAS*, 358, 363
 Clariá, J. J. 2008, Anales de las Primeras Jornadas sobre Astrofísica Estelar, ed. J. J. Clariá, & M. G. Abadi (Córdoba: Observatorio de Córdoba), 39
 Clariá, J. J., Parisi, M. C., Ahumada, A. V., Jr., Santos, J. F. C., Bica, E., & Piatti, A. E. 2007, in IAU Symp. 241, Stellar Populations as Building Blocks of Galaxies (Cambridge: Cambridge Univ. Press), 327
 Clariá, J. J., Piatti, A. E., Mermilliod, J.-C., & Parisi, M. C. 2006, *A&A*, 453, 91
 Dias, B., Coelho, P., Barbuy, B., Kerber, L., & Idiart, T. 2010, *A&A*, 520, 85
 Dutra, C. M., Bica, E., Clariá, J. J., Piatti, A. E., & Ahumada, A. V. 2001, *A&A*, 371, 895
 Girardi, L., Bertelli, G., Bressan, A., Chiosi, C., Groenewegen, M. A. T., et al. 2002, *A&A*, 391, 195
 Gunn, J. E., & Stryker, L. L. 1983, *ApJS*, 52, 121
 Hasegawa, T., Sakamoto, T., & Malasan, H. L. 2008, *PASJ*, 60, 1267
 Kurucz, R. L. 1992, in IAU Symp. 149, The Stellar Populations of Galaxies (Dordrecht: Kluwer), 225
 Le Borgne, J., Bruzual, G., Pelló, R., Lancon, A., et al. 2003, *A&A*, 402, 433
 Lejeune, T., & Schaerer, D. 2001, *A&A*, 366, 538
 Lyngå, G. 1987, Catalogue of Open Cluster Data (Strasbourg: Centre de Données Stellaires)
 Mermilliod, J.-C., Clariá, J. J., Andersen, J., Piatti, A. E., & Mayor, M. 2001, *A&A*, 375, 30
 Palma, T., Ahumada, A. V., Clariá, J. J., & Bica, E. 2008a, *Astron. Nachr.*, 329, 392
 Palma, T., Ahumada, A. V., Clariá, J. J., Jr., Santos, J. F. C., & Bica, E. 2008b, *Acta Astron.*, 58, 359
 Piatti, A. E., Bica, E., Clariá, J. J., Jr., Santos, J. F. C., & Ahumada, A. V. 2002, *MNRAS*, 335, 233
 Piatti, A. E., Jr., Santos, J. F. C., Clariá, J. J., Ahumada, A. V., Bica, E., & Parisi, M. C. 2005, *A&A*, 440, 111

- Press, W. H., et al. 2002, Numerical Recipes in C++: The Art of Scientific Computing, (Cambridge: Cambridge Univ. Press)
- Santos, J.F.C., Jr., & Bica, E. 1993, MNRAS, 260, 915
- Santos, J.F.C., Jr., Bica, E., Clariá, J. J., Piatti, A. E., Girardi, L. A., & Dottori, H. 1995, MNRAS, 276, 1155
- Santos, J.F.C., Jr., Clariá, J. J., Ahumada, A. V., Bica, E., Piatti, A. E., & Parisi, M. C. 2006, A&A, 448, 1023
- Scalo, J. 1998, in ASP Conf. Ser. 142, The Stellar Initial Mass Function (San Francisco: ASP), 201
- Schlegel, D. J., Finkbeiner, D. P., & Davis, M. 1998, ApJ, 500, 525
- Seaton, M. J. 1979, MNRAS, 187, 73
- Talavera, M. L., Ahumada, A. V., Santos, J.F.C., Jr., Clariá, J. J., Bica, E., Parisi, M. C., & Torres, M. C. 2010, Astron. Nachr., 331, 323